Physical Interaction between Human And a Bipedal Humanoid Robot
-Realization of Human-follow Walking-

*Samuel Agus SETIAWAN **Sang Ho HYON
***Jin'ichi YAMAGUCHI * ***Atsuo TAKANISHI
*Department of Mechanical Engineering, Waseda University
**Department of Control and Systems Engineering, Tokyo Institute of Technology
***Humanoid Research Laboratory, Advanced Research Institute for Science and Engineering, Waseda University
3-4-1 Okubo, Shinjuku-ku, Tokyo, 169, Japan
E-mail: samuel@mse.waseda.ac.jp

Abstract

This research is aimed at the development of bipedal humanoid robots working in a human living space, with a focus on its physical construction and motion control method. At the first stage, we developed the bipedal humanoid robot WABIAN (WAseda BIpedal humANoid), and proposed a control method for dynamic cooperative biped walking[1]. In this paper, we presented a follow-walking control method with a switching patterns technique for a bipedal humanoid robot to follow human motion by hand contact. By a combination of both algorithms, the robot has been able to perform dynamic stepping, walking forward and backward in a continuos time while someone is pushing or pulling its hand in such a way. In this paper, the authors describe the control methods for the realization of physical interaction between a human and a bipedal humanoid robot.

1. Introduction

Bipedal humanoid robots intended to share the same working space with humans have different functional workability from robots in factories, construction fields, or hazardous environments. They are strongly desired to have a flexible workability, such as doing along with human motion in physical contact.

There are many studies that deal with physical interaction problems in human-robot coexistence [2,3]. However there are no reports on the realization of physical interaction between a human and a life-sized humanoid robot based on various action models.

On the other hand, a physical interaction between humans may be realized by the action of shaking hands, walking together hand in hand, and even dancing. From these cases, it is reasonable to suppose that the hand has an important role in physical interactions with humans. Thus, under the circumstances of human-robot coexistence, our purpose for this research is to realize a locomotive following motion by a bipedal humanoid robot to human motion by hand contact.

In this paper, we first describe the control method of whole body cooperative walking. This control method is used to stabilize the dynamic walking of the robot.

To let WABIAN follow human guidance motions, we proposed a new follow-walking control method. This method contains three parts, i.e.: 1) upper-limb (arm) following control method, to let the robot's hand follow to the direction of the guidance motion, 2) lower-limb trajectory planning method, to let the robot walk (or just marching in place) in the direction of its guidance motion, 3) trunk trajectory planning method, to compensate for the moment generated by upper and lower limbs. Yet, it is difficult to calculate the trunk trajectory for compensation (no.3), due to the non-linearity of the equation of motion for a bipedal robot. In the next section, we propose a new control method called the human-follow walking with switching patterns technique. This method calculates the joint trajectories, including the trunk trajectory for the compensation of various motion patterns generated offline. Then it provides them as the selectable preset walking patterns for real-time motion.

Finally, we show that by the combination of both control methods, WABIAN can follow human motion when someone is pulling or pushing its hand.

2. Control Method of Dynamic Cooperative Walking

The walking control method is an improved version of a model based walking control with compensation for three-axis moment by trunk motion, which has been applied to our former bipedal robot WL-12RV[4]. In the first stage of development, this control method only puts an emphasis on the consideration of the upper-limb's model on its moment calculation algorithm with a presupposition of fixed order of priority. In brief, this algorithm computes the compensatory trunk motion from the motion of the lower-limbs, the time trajectory of ZMP, and the time trajectory of the hands. This algorithm consists of the following four main parts.

(1) Modeling of the robot

(2) Derivation of the ZMP equations
(3) Computation of approximate trunk motion
(4) Computation of strict trunk motion by iteratively computing the approximate trunk motion

The other component of the control method is a program control for walking using preset walking patterns transformed from the motion of the lower-limbs, trunk, and upper-limbs.

In this section, we describe the algorithm for computing the compensatory trunk motion.

2.1 Modeling of the Robot

Let the walking system be assumed as follows:

(1) The robot is a system of particles.
(2) The floor for walking is solid and not moved by any force or moment.
(3) A Cartesian coordinate system is determined as shown in **Fig.1**. Here, the X-axis and Y-axis form a plane which is the same as that of the floor.
(4) The contact region between the foot and the floor is a set of contact points.
(5) The coefficient of friction for rotation around the X, Y and Z-axes is zero at the contact point.

2.2 Derivation of the ZMP Equations and Computation of Trunk Motion

By assuming that the upper-limb is one part of the trunk (**Fig.2**), we could first define an approximation model of the trunk and the position vectors as shown in **Fig.3**. Based on this model and the D'lambert principle, the moment balance around a point P on the floor can be expressed as below:

$$m_{T1} r_{T1}' \times \ddot{r}_{T1}' + \sum_{i}^{all\_particles} m_i(\mathbf{r}_i - p) \times (\ddot{\mathbf{r}}_i + \mathbf{G}) + \mathbf{T} = \mathbf{0} \quad (1)$$

Point P is defined as ZMP, so we denote the position vector of P as $P_{zmp}(x_{zmp}, y_{zmp}, 0)$. To consider the relative motion of each part, a translational moving coordinate $\overline{W}$-$\overline{XYZ}$ is

$$\begin{aligned} & m_{T1}(z_T'\ddot{x}_T' - x_T'\ddot{z}_T') + m_T(\bar{z}_T + z_q)(\ddot{\bar{x}}_T + \ddot{x}_q) \\ & - m_T(\ddot{\bar{z}}_T + \ddot{z}_q + g)(\bar{x}_T - \bar{x}_{zmp}) = -My(t) \end{aligned} \quad (2)$$

$$\begin{aligned} & m_{T1}(y_T'\ddot{z}_T' - z_T'\ddot{y}_T') - m_T(\bar{z}_T + z_q)(\ddot{\bar{y}}_T + \ddot{y}_q) \\ & + m_T(\ddot{\bar{z}}_T + \ddot{z}_q + g)(\bar{y}_T - \bar{y}_{zmp}) = -Mx(t) \end{aligned} \quad (3)$$

$$m_{T1}(x_T'\ddot{y}_T' - y_T'\ddot{x}_T') + Mz_T(t) = -Mz(t) \quad (4)$$

$$\begin{aligned} Mz_T(t) = & -m_T(\ddot{\bar{x}}_T + \ddot{x}_q)(\bar{y}_T - \bar{y}_{zmp}) \\ & + m_T(\ddot{\bar{y}}_T + \ddot{y}_q)(\bar{x}_T - x_{zmp}) \end{aligned} \quad (5)$$

established on the waist of the robot on a parallel with the fixed coordinate O-XYZ (shown in Fig. 1). $Q(x_q, y_q, z_q)$ is defined as the origin of $\overline{W}$-$\overline{XYZ}$ on the O-XYZ. Using the coordinate $\overline{W}$-$\overline{XYZ}$, equation (1) can be modified and expanded into (2), (3), (4), (5) by putting the terms about the motion of the upper-limb particles on the left-hand side as unknown variables, and the terms about the moment generated by the lower-limb particles on the right-hand side as known

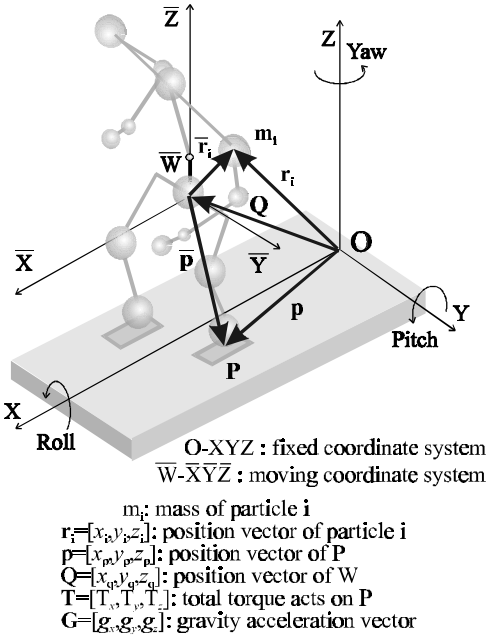

Fig. 1 Definition of coordinate system and vector

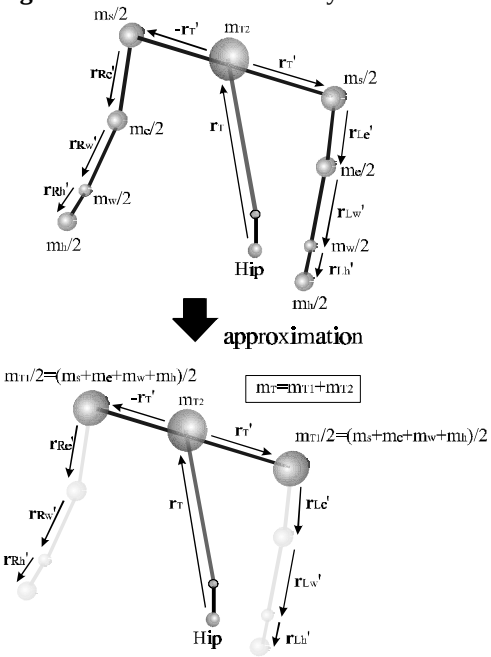

Fig. 2 Approximation model of upper part

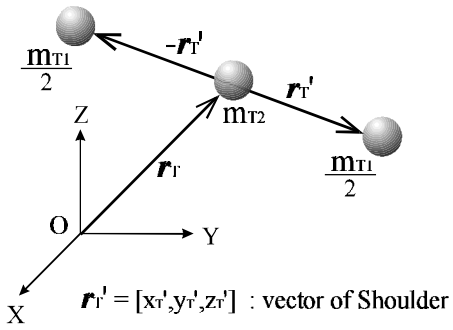

$m_T = m_{T1} + m_{T2}$

Fig. 3 Definition of position vectors for trunk

parameters, named $M(Mx, My, Mz)$ respectively.

However, these equations are interferential and non-linear, because each equation has the same variable, z_T and the trunk is connected to the lower-limbs by rotational joints. Therefore, it is difficult to derive analytic solutions from them. Thus, the other stage of approximation is needed. By assuming that neither the waist nor the trunk particles move vertically, i.e., the trunk arm rotates on the horizontal plane only, the equations can be decoupled and linearized. The yaw-axis moment generated by the yaw-axis actuator is described by the rotational angle of the yaw-axis actuator q_y and the radius of the trunk's arm R, and the linearized equations (6), (7) and (8) are thereby obtained.

$$m_T(\bar{z}_T + z_q)(\ddot{\bar{x}}_T + \ddot{x}_q) - m_T g(\bar{x}_T - \bar{x}_{zmp}) = -My \quad (6)$$

$$-m_T(\bar{z}_T + z_q)(\ddot{\bar{y}}_T + \ddot{y}_q) - m_T g(\bar{y}_T - \bar{y}_{zmp}) = -Mx \quad (7)$$

$$m_{T1}R^2 q_y = -Mz_0 - Mz \quad (8)$$

In these equations, My, Mx, Mz are known, because they are derived from the lower-limb's motion and the time trajectory of ZMP. Also, yaw-axis moment generated by the trunk motion Mz_0 is derived from the pitch and roll-axis motion of the trunk. In the case of steady walking, My, Mx, Mz are periodic functions, because each particle of the lower-limbs and the time trajectory of ZMP move periodically for the moving coordinate $\overline{W}$ - $\overline{X}\overline{Y}\overline{Z}$. Thus, each equation can be represented as a Fourier series. By comparing the Fourier Transform coefficients from both sides of each equation, we can easily acquire the approximate periodic solution for trunk motion. To determine an offset term in the equation of the yaw-axis moment, we take into consideration that the generated yaw-motion angle is in the range of the rotatable region of the yaw-axis actuator.

The above computation is applicable not only to steady walking, but also to complete walking. That is, by regarding complete walking as one walking cycle, and making static

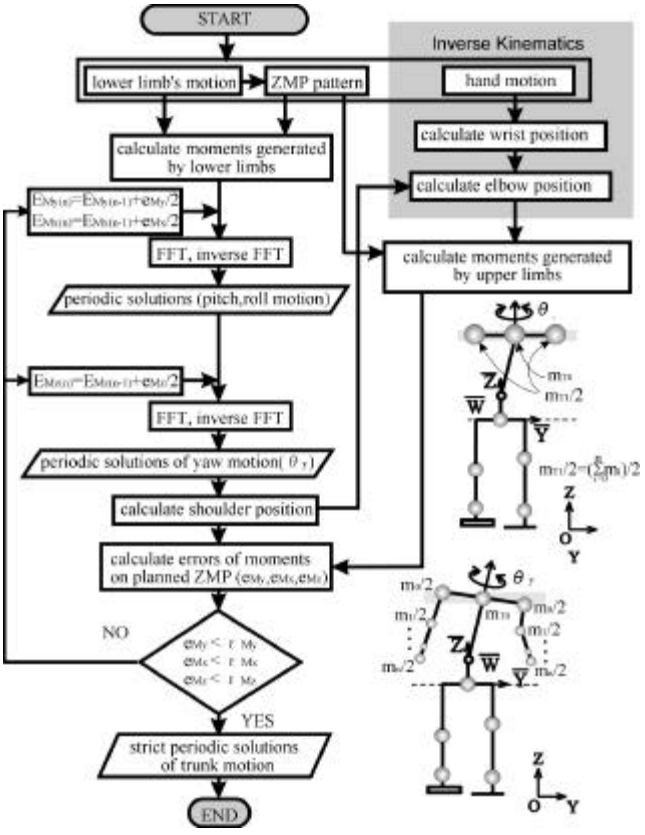

Fig. 4 Flow chart to compute trunk motion

standing states before and after walking long enough, we could apply the algorithm to it.

Further, in order to compute strict solutions, we proposed an algorithm that computes the approximate solutions iteratively. The flowchart of the algorithm is shown in **Fig.4**. $e(e_{My}, e_{Mx}, e_{Mz})$ determines a specific tolerance level of moment error. However, this method needs a huge number of iterations in computation. So, through the use of computation regularity, we used (9) to estimate the limit value of an accumulated moment error for each axis. As a consequence, we realized about a 90 percent decrease in the number of iteration times.

$$E_n = \frac{2E_{(n-1)} + e_{(n-1)}}{2} \quad (9)$$

$$n = 3,4,5, \quad \cdots$$

$$where\, E_1 = 0, E_2 = e_1$$

$E_n(E_{My(t)}, E_{Mx(t)}, E_{Mz(t)})$ is the accumulated moment error in the n-th iteration, and e_n is the calculated moment error after n times of iterations.

3. Control Method for Human-follow Motion.

We applied virtual compliance control to let the robot's arm follow human motion by hand contact. We will adopt a method used by Hirabayashi et al.[6]. By this method, the compliance motion equation of the robot hand is expressed by:

$$M\frac{d\bar{v}}{dt} = \bar{f} - K\Delta\bar{x} - C\bar{v} \qquad (10)$$

where M (6x6 diagonal matrix) is the virtual mass matrix, K (6x6 diagonal matrix) is the stiffness coefficient matrix, C (6x6 diagonal matrix) is the viscosity coefficient matrix, f (6x1 matrix) is the vector of external force act on the robot hand, v (6x1 matrix) is the velocity vector, and x (6x1 matrix) is the hand deviation vector. We set the robot arm coordinate system as shown in **Fig.5**.

In the case where our target is the full tracking ability of the hand, —just like method generally used in the direct teaching of a manipulator—we may disregard the stiffness component. Also, when the control loop time we apply is very short (5[msec]), we may think of the virtual mass as equal to zero. Thus, we can rewrite Eq. (10) in a simply way, i.e.:

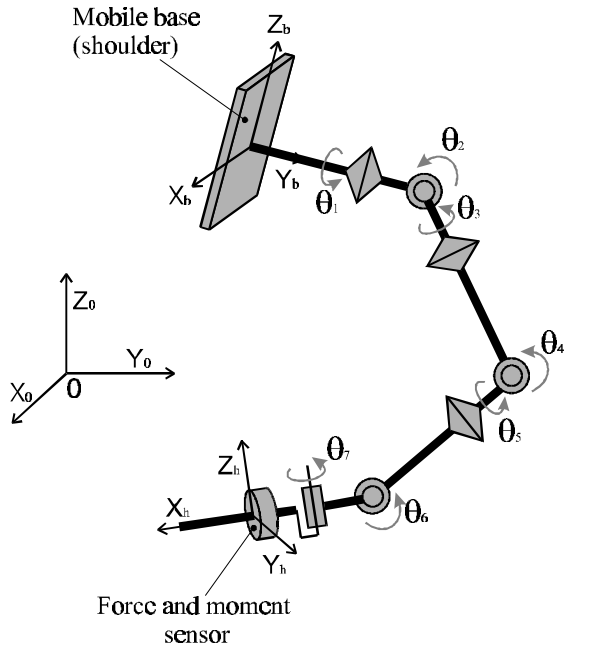

Fig. 5 The upper-limb (arm) model of WABIAN

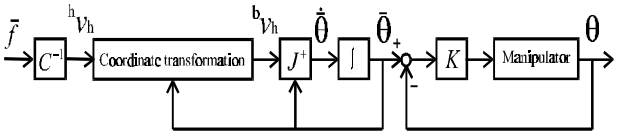

Fig. 6 Control system for the upper-limb's following motion

$$\bar{v} = C^{-1}\bar{f} \qquad (11)$$

According to the redundancy of WABIAN's arm, we used the pseudo-inverse matrix method to calculate the joint angle velocity from the hand velocity. **Fig.6** shows the block diagram of the control system for the upper-limb's following motion. Here, J^+ (6x6 matrix) is the pseudo-inverse matrix.

4. Human-follow Walking Control with Pattern Switching Method

As mentioned above, to realize human-follow walking motion by a bipedal robot, we proposed a new method called the human-follow walking control with pattern switching technique. This method tries to realize a follow-walking motion by selecting and generating changeable unit patterns, based on an action model of human-robot interaction. Note that the selectable unit patterns are calculated offline and kept in the computer memory.

In this section, we will describe the making of unit patterns and decision for the following direction (action model).

4.1 Making of unit patterns

Two men who adjust their motion to one another while moving on the ground, have various gaits while in action. They walk freely in a two-dimensional space, and switch their step or velocity half unconsciously to follow their partner's motion. It is difficult to apply all motion patterns to a bipedal robot. However, by combining some of the selective patterns, it is possible to realize a following motion by a bipedal robot similar to a human's.

By considerating that WABIAN only has pitch direction DOF on its lower-limb, in this research, we only made back and forth (including marching in place) motion patterns for realizing the human-follow motion. However, it can be easily extended to another kind of two-dimensional motion, including sideways or diagonal motions.

There are various numbers of gait patterns even in a back-and-forth motion, and those have a countless number of classification methods. But notice that we can plan the lower-limb motion arbitrarily, while we can only decide the trunk trajectory due to consideration of the dynamical condition of balance of the robot. We are able to make and classify various kinds of motion patterns after from the observation explained below.

4.1.1 Classification of unit patterns of the lower-limb

By defining a step of back-and-forth walking as a unit pattern, we classified the motion of each leg into five types of step motion in consideration of the locomotive motion

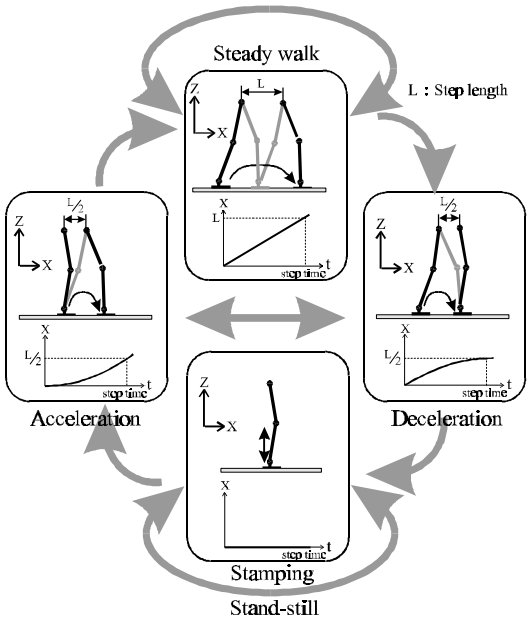

Fig. 7 Lower-limb's motion divided into 5 types of step

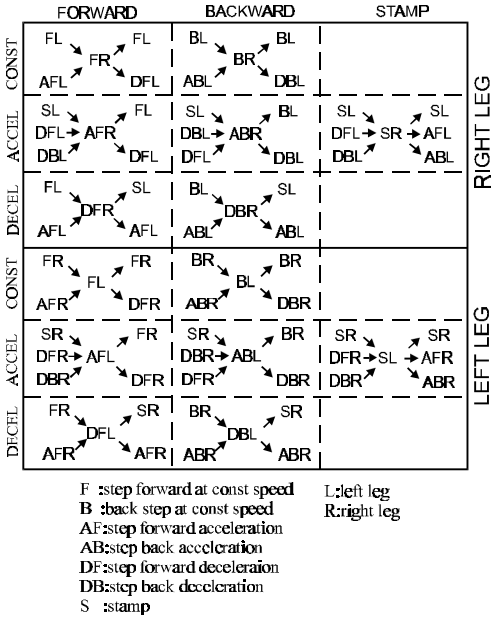

Fig. 8 Connection rule of the unit patterns

velocity (gait attribute per step) as shown in **Fig.7**.

Basically, we realized the human-follow motion by the combination of these types of step motions. To prevent unstability in the trajectory of the trunk (explained in the next section), caused by an excessive change of moment around the ZMP, we decided that the lower-limb unit patterns must be performed mutually in the direction of the arrow in Fig.7. The connection rule for the unit patterns is shown in **Fig.8**.

4.1.2 Classification of unit patterns of the trunk

We planned the trunk trajectory to compensate for the moment generated by the lower-limb motion planned above.

It has been noted that in classifying unit patterns of the trunk, the dynamics of the trunk motion should be considered. We can deform the equation of moment balance around the pitch and roll axis (Eq.6 & 7) as below:

$$(\bar{z}_T + z_q)\ddot{\bar{x}}_T - g\bar{x}_T = \Phi(t) \quad (12)$$

$$(\bar{z}_T + z_q)\ddot{\bar{y}}_T - g\bar{y}_T = \Psi(t) \quad (13)$$

where $\Phi(t)$ and $\Psi(t)$ are known variables in the equation (6) and (7).

Here, we simply discuss the trunk motion around the pitch axis. The transfer function in the frequency domain of equation (12) can be expressed as below:

$$g(w) = \frac{2a}{w^2 + a^2} b = \left(\frac{1}{a - jw} + \frac{1}{a + jw}\right) b \quad (14)$$

where,

$$a = \sqrt{\frac{g}{(\bar{z}_T + z_q)}}, \quad b = -\frac{1}{2g}\sqrt{\frac{g}{(\bar{z}_T + z_q)}}$$

Equation (14) is generally known as the Lorentz Function, and its primitive function is, i.e.:

$$g(t) = be^{-a|t|} \quad (15)$$

Fig.9 shows the impulse response of $\Phi(t)$. We could see that the causal law is not approved anymore in this case. Thus, it should be clear that the trunk compensation motion occurs earlier than the shift of ZMP on the floor. It also means that the trunk compensation gives effect to one or more steps before and after in a pattern time. The frequency of the trunk moment is higher as the

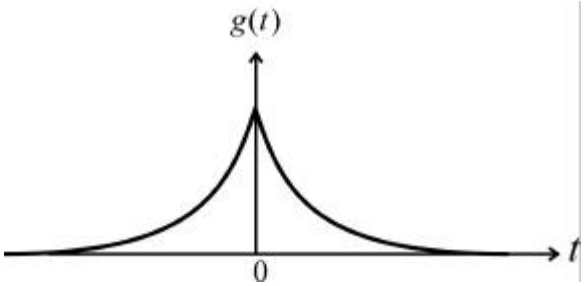

Fig. 9 Impulse response of Eq.(12)

	prev	curr	next
	A		
0	FL	FR	FL
1	AFL	FR	FL
2	FL	FR	DFL
3	AFL	FR	DFL
	B		
4	SL	AFR	FL
5	DFL	AFR	FL
6	DBL	AFR	FL
7	IDLE	AFR	FL
8	SL	AFR	DFL
9	DFL	AFR	DFL
10	DBL	AFR	DFL
11	IDLE	AFR	DFL
	C		
12	FL	DFR	SL
13	AFL	DFR	SL
14	FL	DFR	AFL
15	AFL	DFR	AFL
16	FL	DFR	ABL
17	AFL	DFR	ABL
18	FL	DFR	IDLE
19	AFL	DFR	IDLE

	prev	curr	next
	D		
20	BL	BR	BL
21	ABL	BR	BL
22	BL	BR	DBL
23	ABL	BR	DBL
	E		
24	SL	ABR	BL
25	DBL	ABR	BL
26	DFL	ABR	BL
27	IDLE	ABR	BL
28	SL	ABR	DBL
29	DBL	ABR	DBL
30	DFL	ABR	DBL
31	IDLE	ABR	DBL
	F		
32	BL	DBR	SL
33	ABL	DBR	SL
34	BL	DBR	ABL
35	ABL	DBR	ABL
36	BL	DBR	AFL
37	ABL	DBR	AFL
38	BL	DBR	IDLE
39	ABL	DBR	IDLE

	prev	curr	next
	G		
40	FR	FL	FR
41	AFR	FL	FR
42	FR	FL	DFR
43	AFR	FL	DFR
	H		
44	SR	AFL	FR
45	DFR	AFL	FR
46	DBR	AFL	FR
47	IDLE	AFL	FR
48	SR	AFL	DFR
49	DFR	AFL	DFR
50	DBR	AFL	DFR
51	IDLE	AFL	DFR
	I		
52	FR	DFL	SR
53	AFR	DFL	SR
54	FR	DFL	AFR
55	AFR	DFL	AFR
56	FR	DFL	ABR
57	AFR	DFL	ABR
58	FR	DFL	IDLE
59	AFR	DFL	IDLE

	prev	curr	next
	J		
60	BR	BL	BR
61	ABR	BL	BR
62	BR	BL	DBR
63	ABR	BL	DBR
	K		
64	SR	ABL	BR
65	DBR	ABL	BR
66	DFR	ABL	BR
67	IDLE	ABL	BR
68	SR	ABL	DBR
69	DBR	ABL	DBR
70	DFR	ABL	DBR
71	IDLE	ABL	DBR
	L		
72	BR	DBL	SR
73	ABR	DBL	SR
74	BR	DBL	ABR
75	ABR	DBL	ABR
76	BR	DBL	AFR
77	ABR	DBL	AFR
78	BR	DBL	IDLE
79	ABR	DBL	IDLE

	prev	curr	next
	M		
80	SL	SR	SL
81	DFL	SR	SL
82	DBL	SR	SL
83	IDLE	SR	SL
84	SL	SR	AFL
85	DFL	SR	AFL
86	DBL	SR	AFL
87	IDLE	SR	AFL
88	SL	SR	ABL
89	DBL	SR	ABL
90	DFL	SR	ABL
91	IDLE	SR	ABL
92	SL	SR	IDLE
93	DFL	SR	IDLE
94	DBL	SR	IDLE

	prev	curr	next
	N		
95	SR	SL	SR
96	DFR	SL	SR
97	DBR	SL	SR
98	IDLE	SL	SR
99	SR	SL	AFR
100	DFR	SL	AFR
101	DBR	SL	AFR
102	IDLE	SL	AFR
103	SR	SL	ABR
104	DBR	SL	ABR
105	DFR	SL	ABR
106	IDLE	SL	ABR
107	SR	SL	IDLE
108	DFR	SL	IDLE
109	DBR	SL	IDLE

F:step forward at const speed
B:step back at const speed
AF:step forward acceleration
AB:step back acceleration
DF:step forward deceleration
DB:step back deceleration
IDLE:idling(stand still)
S:stamp
R:right leg
L:left leg

Fig. 10 Unit walking pattern

robot moves faster, therefore the effect of g(*w*) is more dominant in a fast motion.

From a simulation, we have confirmed that even during high speed motion (±1.0[sec/step]), it is possible to make a unit pattern for the trunk by taking into account only one step before and after as an attribute.

By using a simulator, we made unit patterns of the lower-limb and trunk based on the consideration above. The unit patterns created contain indexes for pattern searching and attributes of steps current, before and after, as shown in **Fig.10**. These patterns are preloaded as one step long angle data in the memory.

4.1.3 Decision of following direction

In this section, we will discuss a topic equivalent to a part of the action model in human physical interaction. That is, a process where a robot recognizes human intention, then decides to start an action as a response.

Under the circumstances of interaction between a human and his/her partner, including the surrounding environment, there is a mapping process (an action model of a behavioural pattern) between the conditions of three elements that change depending on the time and action to be performed. Based on this consideration, we determined an action model to realize the interaction between a human and a bipedal robot as shown in **Fig.11**. In this model, the robot recognizes the guiding direction of the human to move by detecting the position or displacement of its hand, and decides the next walking pattern while synchronizing it with the present walking condition. In the case of where no pattern is selected, we programmed to let the present condition be continued by the robot.

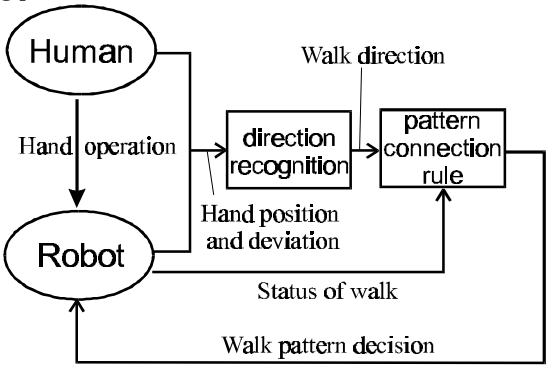

Recognition of the walk direction by the hand position

$X_{back} \le x_h \le X_{forward}$ *and* $\Delta x_h \le D$ → STOP

$X_{back} < x_h$ *and* $D < \Delta x_h$ → FORWARD

$x_h < X_{forward}$ *and* $\Delta x_h < D$ → BACK

x_h Hand position
Δx_h Hand deviation
$X_{forward}$ Position limit(forward)
X_{back} Position limit(back)
D Deviation limit

Fig. 11 The interaction model

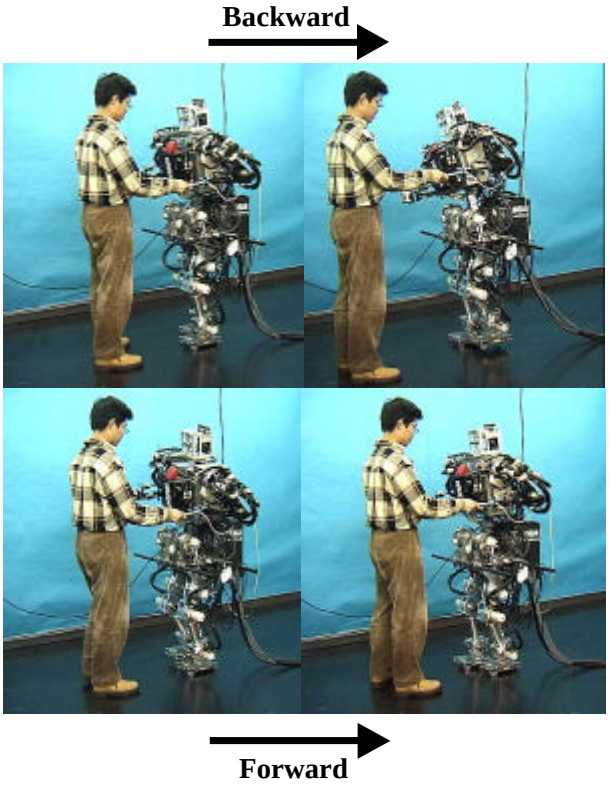

Fig. 12 A scene of physical experiment with WABIAN

5. Experiment

To perform human-follow experiments with WABIAN, we installed a six-axis moment and force sensor on its wrist. We proposed a human-follow walking experiment with 16 steps using WABIAN. The step velocity is 1.28[s/step], the step width is 0.1[m], and the inverse viscosity coefficient for compliance is 0.15 [m/Ns] (**Table 1**). **Fig. 12** shows a cut of a scene of the experiment.

parameter	value
X_{foward}	0.3
X_{back}	0.1
D	0.15

Table 1 Parameters for the experiment

6. Conclusions and Future Works

In this research, we presented a control technique to realize physical interaction between a human and a life-size humanoid robot based on an action model. We proposed a follow-walking method based on a previously developed dynamic cooperative walking algorithm, to let a bipedal robot follow human guidance motions through hand contact.

We revised our bipedal robot WABIAN by installing a new six-axis moment and force sensor system on its wrist. Then, we performed a human-follow walking experiment using this system and the newly developed control technique.

In the near future, we will expand our work to full 2 dimensional motion, including sideways, diagonal walkings or turning. We have developed a bipedal humanoid robot WABIAN-R (WAseda BIpedal humANoid-Revised), which has six DOF on each leg to enable it to realize more various motions, not even in a two-dimensional space but also in a three-dimensional space. We will introduce our work on the new bipedal humanoid robot at another chance.

Acknowledgment

This study has been conducted as a part of the project: Humanoid at HUREL (HUmanoid REsearch Laboratory), Advanced Research Institute for Science and Engineering, Waseda University. The authors would like to thank ATR, NAMCO Ltd., YASKAWA ELECTRIC Corp., NISSAN MOTOR CO., LTD., and NIPPON STEEL CORPORATION for their cooperation in this study. A part of this study was done by the Japanese Grant-in-Aid for Science Research (No. 07405012) and NEDO (New Energy and Industrial Technology Development Organization).

The authors would also like to thank NITTA Corp, OKINO Industries ltd., Harmonic Drive Systems, Inc., YKK Corp, Daisuke AOYAGI and Akihiro NAGAMATSU for supporting us in developing the hardware for the six-axis moment and force sensor system.

References

[1] J. Yamaguchi, S. Inoue, D. Nishino, A. Takanishi “Development of a Bipedal Robot Having Antagonistic Joints and Three DOF Trunk”, Proc. of the 1998 IROS, pp. 96-101, 1998

[2] Q. Huang, S. Sugano “Motion Planning of Stabilization and Cooperation of a Mobile Manipulator”, Proc. of the 1996 ICRA, pp. 568-575, 1996

[3] H. Kazerooni “Human-Robot Interaction via the Transfer of Power and Information Signals”, IEEE Trans. on SMC, Vol. 20, No.2, pp.450-463,1990

[4] J. Yamaguchi, A. Takanishi, I. Kato “Development of a Biped Walking Robot Compensating for Three-Axis Moment by Trunk Motion”, Proc. of IROS’93, pp. 561-566, 1993

[5] T. Yoshikawa “Analysis and Control of Robot Manipulators with Redundancy”, Robotics Research, MIT Press, 1984

[6] M. T. Mason “Compliance and Force Control for Computer Controlled Manipulators”, IEEE Trans. on SMC, Vol.11, No.6, pp.418-432, 1981

[7] H. Hirabayashi, K. Sugimoto, S. Arai, S. Sakaue “Virtual Compliance Control of Multiple Degree of Freedom Robot”, (in Japanese), Proc. of SICE’85, pp. 343-350, 1985

[8] Y. Kuniyoshi, A. Nagakubo “Humanoid Interaction Research –Towards Emergence of Three-Term Interaction Among Human, Robot and Environment”, Proc. of 14th RSJ’96, pp. 711-712, 1996